

Article

Classical and relativistic evolution of an extra-galactic jet with back-reaction

Lorenzo Zaninetti ¹,¹ Department of Physics, University of Turin, via P.Giuria 1,
I-10125 Turin, Italy*Version March 10, 2024 submitted to Galaxies. Typeset by L^AT_EX using class file mdpi.cls*

Abstract: We consider a turbulent jet which is moving in a Lane–Emden ($n = 5$) medium. The conserved quantity is the energy flux, which allows finding, to first order, an analytical expression for the velocity and an approximate trajectory. The conservation of the relativistic flux for the energy allows deriving, to first order, an analytical expression for the velocity, and numerically determining the trajectory. The back-reaction due to the radiative losses for the trajectory is evaluated both in the classical and the relativistic case.

Keywords: Radio galaxies; Jets and bursts; galactic winds and fountains Radio sources

PACS classifications: 98.54.Gr 98.62.Nx 98.70.Dk

1. Introduction

The study of extra-galactic jets started with the observations of NGC 4486 (M87), where ‘a curious straight ray lies in a sharp gap in the nebulosity ...’, see [1] and Figure 1. At the moment of writing, the extra-galactic radio sources are classified on the basis of the position of the brightest radio emitting regions with respect to the channel, see [2,3] for details. FR-I, after Fanaroff & Riley, have hot spots that are more distant from the nucleus (a typical example is Cygnus A) and luminosity, L , at 178 Mhz of

$$L \leq h_{100} 2 \cdot 10^{25} \frac{W}{Hz \text{ str}} \quad \text{FR-I} \quad , \quad (1)$$

where $h_{100} = H_0/100$ and H_0 is the Hubble constant. FR-II radio galaxies have emission uniformly distributed along the channel (typical example 3C449) and luminosities greater than the above value or, in other words, the more powerful radio galaxies are classified as FR-II. A list of the properties, length in



Figure 1. The super-giant elliptical galaxy M87 and the optical jet; the credit is due to Instituto de Astrofísica de Canarias.

13 kpc and power in Watt, of extra-galactic radio jets can be found in [4,5]. In the following we will study
 14 jets with small openings, such as that of M87.

15 The problem of the velocity of extra-galactic radio jets has been analysed in two ways:

- 16 1. The velocity of the jet is constant over many kpc and takes the value v . Due to the fact that is
 17 thought that this velocity is nearly relativistic, it is parametrized as $\beta = \frac{v}{c}$, where c is the velocity
 18 of light. As an example, [6] analysed some wide-angle tail radio galaxies and found a terminal
 19 velocity of $\beta = 0.3$.
- 20 2. The velocity of the jet decreases with an imposed law, see [7], or is evaluated by a numerical code,
 21 see [8,9]. In this case, the relativistic parameter β decreases along the trajectory.

22 Recently the problem of the decrease of the velocity along a turbulent jet has been solved, imposing the
 23 conservation of the flux of momentum, see [10], or imposing the conservation of the energy flux, see
 24 [11]. The approach using the conservation of the flux of energy is attractive because it has the same
 25 dimension of the luminosity. Further on, the jets are radiating away in the various observational bands,
 26 such as radio, optical, infrared, etc., and we briefly recall that the extra-galactic radio source covers a
 27 range in observed luminosity from $10^{19} \frac{W}{Hz}$ to $10^{28} \frac{W}{Hz}$, see [12].

28 Therefore the flux of energy available at the beginning of the jet will progressively decrease due to
 29 the radiative losses. This paper, in Section 2, introduces the Lane–Emden ($n = 5$) density profile and
 30 consequently derives an approximate trajectory to first order as well as a numerical trajectory to second
 31 order in the presence of losses. In Section 3 we present a series solution for the relativistic trajectory to
 32 first order and a numerical solution to second order. Section 4 models the intensity of the radio-jet in
 33 3C31.

34 2. Conservation of the flux of energy

35 A turbulent jet is defined as a jet which has the same density as the surrounding intergalactic medium
 36 (IGM), see the next subsection for details. The conservation of the flux of energy in a turbulent jet has
 37 been explored in [11] for three types of IGM, with the following radial dependences: constant density

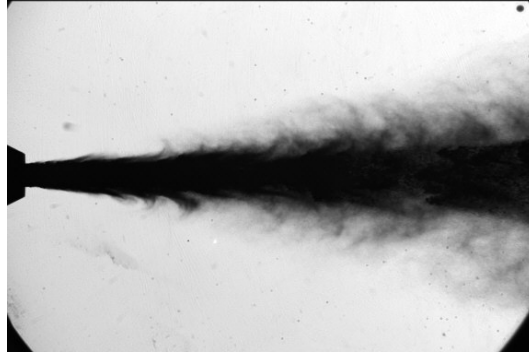


Figure 2. Coaxial liquid-air jet; the credit is due to Mixing Enhancement via Secondary Parallel Injection (MESPI).

38 profile, hyperbolic and inverse power law density profiles. Here we analyse the case of a Lane–Emden
39 ($n=5$) density profile, to which a subsection will be dedicated.

40 2.1. The turbulent jet

41 Turbulent jets are a subject of laboratory experiments, as an example, see Figure 2. The theory of
42 turbulent jets emerging from a circular hole can be found in different books with different theories, see
43 [13], [14], and [15]. The basic assumptions common to the three already cited approaches are

1. The rate of momentum flow, J , represented by

$$J = \text{constant} \times \rho b_j^2 \bar{v}_{x,max}^2 \quad , \quad (2)$$

is constant; here x is the distance from the initial circular hole, $b_j(x)$ is the jet's diameter at distance x , $\bar{v}_{x,max}$ is the maximum velocity along the the centreline, constant is

$$\text{constant} = 2\pi \int_0^\infty f^2 \xi d\xi \quad , \quad (3)$$

where

$$f(\xi) = \frac{\bar{v}_x}{\bar{v}_{x,max}} \quad \text{with} \quad \xi = \frac{x}{b_{1/2}} \quad , \quad (4)$$

44 and ρ is the density of the surrounding medium, see equation (5.6-3) in [13].

- 45 2. The jet's density ρ is constant over the expansion and equal to that of the surrounding medium.
46 The pressure is absent in this theory.

Omitting the details of the computation, an expression can be found for the average velocity \bar{v}_x , see equation (5.6-21) in [13],

$$\bar{v}_x = \frac{\nu^{(t)}}{x} \frac{2C_3^2}{\left[1 + \frac{1}{4}(C_3 \frac{r}{x})^2\right]^2} \quad , \quad (5)$$

where $\nu^{(t)}$ is the kinematical eddy viscosity and C_3 is as follows, see equation (5.6-23) in [13],

$$C_3 = \sqrt{\frac{3}{16\pi}} \sqrt{\frac{J}{\rho}} \frac{1}{\nu^{(t)}} \quad . \quad (6)$$

An important quantity is the radial position, $r = b_{1/2}$, corresponding to an axial velocity one-half of the centreline value, see equation (5.6-24) in [13],

$$\frac{\bar{v}_x(b_{1/2}, x)}{\bar{v}_{x,max}(x)} = \frac{1}{2} = \frac{1}{\left[1 + \frac{1}{4}(C_3 \frac{b_{1/2}}{x})^2\right]^2} \quad . \quad (7)$$

The experiments in the range of Reynolds number, Re , $10^4 \leq Re \leq 310^6$ (see [16], [17] and [18]) indicate that

$$b_{1/2} = 0.0848x \quad , \quad (8)$$

and as a consequence

$$C_3 = 15.17 \quad , \quad (9)$$

and therefore

$$\frac{\bar{v}_x(r)}{\bar{v}_{x,max}(r)} = \frac{1}{\left[1 + 0.414\left(\frac{r}{b_{1/2}}\right)^2\right]^2} \quad . \quad (10)$$

The average velocity, \bar{v}_x , is $\approx 1/100$ of the centreline value when $r/b_{1/2} = 4.6$ and this allows seeing that the diameter of the jet is

$$b_j = 2 \times 4.6b_{1/2} \quad . \quad (11)$$

On introducing the opening angle α , the following new relation is found:

$$\frac{\alpha}{2} = \arctan \frac{4.6b_{1/2}}{x} \quad . \quad (12)$$

The generally accepted relation between the opening angle and Mach number, see equation (A33) in [19], is

$$\frac{\alpha}{2} = \frac{c_s}{v_j} = \frac{1}{M} \quad , \quad (13)$$

where c_s is the velocity of sound, v_j the jet's velocity, and M the Mach number. The new relation (12) replaces the traditional relation (13). The parameter $b_{1/2}$ can therefore be connected with the jet's geometry:

$$b_{1/2} = \frac{1}{4.6} \tan\left(\frac{\alpha}{2}\right)x \quad . \quad (14)$$

If this approximate theory is accepted, equation (8) gives $\alpha = 42.61^\circ$: this is the theoretical value that yields the so called Reichardt profiles. The value of $b_{1/2}$ fixes the value of C_3 and therefore the eddy viscosity is

$$\nu^{(t)} = \sqrt{\frac{3}{16\pi}} \sqrt{\frac{J}{\rho} \frac{1}{C_3}} = \sqrt{\frac{3}{16\pi}} \sqrt{constant} b v_{x,max} \frac{1}{C_3} \quad . \quad (15)$$

In order to continue, the integral that appears in *constant* should be evaluated, see equation (3). Numerical integration gives

$$\int_0^\infty f^2 \xi d\xi = 0.402 \quad , \quad (16)$$

and therefore

$$constant = 2.528 \quad . \quad (17)$$

On introducing typical parameters of jets like $\alpha=5^\circ$, $v_{x,max}=v_{100} = v[\text{km/sec}]/100$, $b_j = b_1$, where b_1 is the momentary diameter in pc, it is possible to deduce an astrophysical formula for the kinematical eddy viscosity:

$$\nu^{(t)} = 2.92 \cdot 10^{-9} b_1 v_{100} \frac{\text{pc}^2}{\text{year}} \quad \text{when} \quad C_3 = 135.61 \quad . \quad (18)$$

47 This paragraph concludes by underlining the fact that in extra-galactic sources it is possible to observe
48 both a small opening angle, $\approx 5^\circ$ and great opening angles, i.e. $\approx 34^\circ$ in the outer regions of 3C31
49 [20].

50 2.2. The Lane–Emden profile

The self gravitating sphere of a polytropic gas is governed by the Lane–Emden differential equation of the second order

$$\frac{d^2}{dx^2} Y(x) + 2 \frac{\frac{d}{dx} Y(x)}{x} + (Y(x))^n = 0 \quad ,$$

where n is an integer, see [21–25]. The solution $Y(x)_n$ has the density profile

$$\rho = \rho_c Y(x)_n^n \quad ,$$

where ρ_c is the density at $x = 0$. The pressure P and temperature T scale as

$$P = K \rho^{1+\frac{1}{n}} \quad , \quad (19)$$

$$T = K' Y(x) \quad , \quad (20)$$

51 where K and K' are two constants. For more details, see [26].

Analytical solutions exist for $n = 0, 1$, and 5 . The analytical solution for $n=5$ is

$$Y(x) = \frac{1}{(1 + \frac{x^2}{3})^{1/2}} \quad ,$$

and the density for $n=5$ is

$$\rho(x) = \rho_c \frac{1}{(1 + \frac{x^2}{3})^{5/2}} \quad . \quad (21)$$

The variable x is non-dimensional and we now introduce the new variable $x = r/b$

$$\rho(r; b) = \rho_c \frac{1}{(1 + \frac{r^2}{3b^2})^{5/2}} \quad . \quad (22)$$

52 2.3. Preliminaries

The chosen physical units are pc for length and yr for time; with these units, the initial velocity v_0 is expressed in pc yr^{-1} . When the initial velocity is expressed in km s^{-1} , the multiplicative factor 1.02×10^{-6} should be applied in order to have the velocity expressed in pc yr^{-1} . In these units, the speed of light is $c = 0.306 \text{ pc yr}^{-1}$. The goodness of the approximation of a solution is evaluated through the percentage error, δ , which is

$$\delta = \frac{|x - x_{app}|}{x} \times 100 \quad , \quad (23)$$

53 where x is the analytical or numerical solution and x_{app} the approximate solution, see [27].

54 2.4. Classical solution to first order

The conservation of the energy flux in a straight turbulent jet the concept of the perpendicular section section to the motion along the Cartesian x -axis, A

$$A(r) = \pi r^2 \quad (24)$$

where r is the radius of the jet. The section A at position x_0 is

$$A(x_0) = \pi(x_0 \tan(\frac{\alpha}{2}))^2 \quad (25)$$

where α is the opening angle and x_0 is the initial position on the x -axis. At position x we have

$$A(x) = \pi(x \tan(\frac{\alpha}{2}))^2 \quad (26)$$

The conservation of energy flux states that

$$\frac{1}{2}\rho(x_0)v_0^3A(x_0) = \frac{1}{2}\rho(x)v(x)^3A(x) \quad (27)$$

55 where $v(x)$ is the velocity at position x and $v_0(x_0)$ is the velocity at position x_0 , see Formula A28 in
 56 [19]. We now assume that a Lane–Emden ($n = 5$) density profile is valid, see equation (22). Then the
 57 above conservation law becomes

$$\begin{aligned} & \frac{1}{2}\rho_0v(x)^3\pi x^2\left(\tan\left(\frac{\alpha}{2}\right)\right)^2\left(1+\frac{1}{3}\frac{x^2}{b^2}\right)^{-5/2} \\ &= \frac{1}{2}\rho_0v_0(x_0)^3\pi x_0^2\left(\tan\left(\frac{\alpha}{2}\right)\right)^2\left(1+\frac{1}{3}\frac{x_0^2}{b^2}\right)^{-5/2}, \end{aligned} \quad (28)$$

where $v(x)$ is the velocity at position x , $v_0(x_0)$ is the velocity at position x_0 and α is the opening angle of the jet. The above equation is a cubic equation which has one real root plus two non-real complex conjugate roots. Here and in the following we take into account only the real root. The real analytical solution for the velocity without losses is

$$v(x; b, x_0, v_0) = \frac{v_0(3b^2 + x^2)^{\frac{5}{6}}x_0^{\frac{2}{3}}}{(3b^2 + x_0^2)^{\frac{5}{6}}x^{\frac{2}{3}}} \quad (29)$$

The asymptotic expansion of above velocity, v_a , with respect to the variable x , which means $x \rightarrow \infty$, is

$$v_a(x; b, x_0, v_0) = \frac{v_0x_0^{\frac{2}{3}}(5b^2 + 2x^2)}{2(3b^2 + x_0^2)^{5/6}x} \quad (30)$$

The trajectory can be found by the indefinite integral of the inverse of the velocity as given by equation (29):

$$F(x) = \int \frac{1}{v(x; b, x_0, v_0)} dx = \frac{\sqrt[6]{3}(3b^2 + x_0^2)^{\frac{5}{6}}x^{\frac{5}{3}}{}_2F_1(\frac{5}{6}, \frac{5}{6}; \frac{11}{6}; -\frac{x^2}{3b^2})}{5v_0(b^2)^{5/6}x_0^{2/3}}, \quad (31)$$

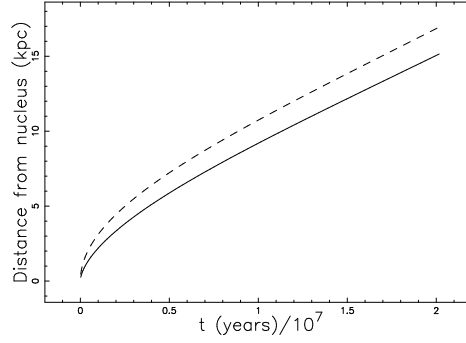


Figure 3. Numerical solution as given by equation (32) (full line) and asymptotic solution as given by equation (35) (dashed line), with parameters as in Table 1.

where ${}_2F_1(a, b; c; v)$ is a regularized hypergeometric function, see [27–30]. The trajectory expressed in terms of t as a function of x is

$$F(x) - F(x_0) = t \quad . \quad (32)$$

The above equation can not be inverted in the usual form, which is x as a function of t . The asymptotic trajectory can be found by the indefinite integral of the inverse of the asymptotic velocity as given by equation (30)

$$F_a(x) = \int \frac{1}{v_a(x; b, x_0, v_0)} dx = \frac{(3b^2 + x_0^2)^{5/6} \ln(5b^2 + 2x^2)}{2v_0x_0^{2/3}} \quad . \quad (33)$$

The equation of the asymptotic trajectory is

$$F_a(x) - F_a(x_0) = t \quad , \quad (34)$$

and the solution for x of the above equation, the asymptotic trajectory, is

$$x(t; b, x_0, v_0) = \frac{1}{2} \sqrt{-10b^2 + 2e^{\frac{(3b^2 + x_0^2)^{5/6} \ln(5b^2 + 2x_0^2) + 2tv_0x_0^{2/3}}{(3b^2 + x_0^2)^{5/6}}}} \quad . \quad (35)$$

58 Figure 3 shows a typical example of the above asymptotic expansion.

Table 1. Parameters for a classical extra-galactic jet.

parameter	value
x_0 (pc)	100
v_0 ($\frac{km}{s}$)	10000
b (pc)	10000

59 2.5. Solution to second order

Let us suppose that the radiative losses are proportional to the flux of energy

$$-\epsilon \frac{\rho_0 v^3 \pi x^2 \left(\tan\left(\frac{\alpha}{2}\right)\right)^2}{2 \left(1 + \frac{1}{3} \frac{x^2}{b^2}\right)^{5/2}} . \quad (36)$$

Inserting in the above equation the velocity to first order as given by equation (29) the radiative losses, $Q(x; x_0, v_0, b, \epsilon)$, are

$$Q(x; x_0, v_0, b, \epsilon) = -\epsilon \frac{\rho_0 v^3 \pi x^2 \left(\tan\left(\frac{\alpha}{2}\right)\right)^2}{2 \left(1 + \frac{1}{3} \frac{x^2}{b^2}\right)^{5/2}} , \quad (37)$$

where ϵ is a constant which fixes the conversion of the flux of energy to other kinds of energies, in this case, the radiative losses. The sum of the radiative losses between x_0 and x is given by the following integral, L ,

$$L(x; x_0, v_0, b, \epsilon) = \int_{x_0}^x Q(x; x_0, v_0, b, \epsilon) dx = \frac{-9\epsilon \rho_0 \sqrt{3} b^5 v_0^3 x_0^2 \pi \left(\tan(\alpha/2)\right)^2 (x - x_0)}{2 (3b^2 + x_0^2)^{5/2}} . \quad (38)$$

60 The conservation of the flux of energy in the presence of the back-reaction due to the radiative losses is

$$\begin{aligned} & \frac{9\sqrt{3}\rho_0 \left(b^5 v_0^3 x_0^2 \epsilon \left(\frac{3b^2+x^2}{b^2} \right)^{5/2} x - b^5 v_0^3 x_0^3 \epsilon \left(\frac{3b^2+x^2}{b^2} \right)^{5/2} + v^3 x^2 (3b^2 + x_0^2)^{5/2} \right)}{2 \left(\frac{3b^2+x^2}{b^2} \right)^{5/2} (3b^2 + x_0^2)^{5/2}} \\ & = 9\rho_0 \sqrt{3} v_0^3 x_0^2 2 \left(\frac{3b^2 + x_0^2}{b^2} \right)^{5/2} . \end{aligned} \quad (39)$$

The analytical solution for the velocity to second order, $v_c(x; b, x_0, v_0)$, is

$$v_c(x; b, x_0, v_0) = \frac{v_0 \sqrt[3]{1 + \epsilon (-x + x_0)} (3b^2 + x^2)^{\frac{5}{6}} x_0^{\frac{2}{3}}}{(3b^2 + x_0^2)^{\frac{5}{6}} x^{\frac{2}{3}}} , \quad (40)$$

61 and Figure 4 shows an example.

62 There are no analytical results for the trajectory corrected for radiative losses, and a numerical
63 example is shown in Figure 5.

The inclusion of back-reaction allows the evaluation of the jet's length, which can be derived from the minimum in the corrected velocity to second order as a function of x ,

$$\frac{\partial v_c(x; b, x_0, v_0)}{\partial x} = 0 , \quad (41)$$

64 which is

$$\begin{aligned} & -\frac{v_0 \epsilon}{3} (3b^2 + x^2)^{\frac{5}{6}} x_0^{\frac{2}{3}} (1 + \epsilon (-x + x_0))^{-\frac{2}{3}} (3b^2 + x_0^2)^{-\frac{5}{6}} x^{-\frac{2}{3}} \\ & + \frac{5v_0}{3} \sqrt[3]{1 + \epsilon (-x + x_0)} x_0^{\frac{2}{3}} \sqrt[3]{x} (3b^2 + x_0^2)^{-\frac{5}{6}} \frac{1}{\sqrt[6]{3b^2 + x^2}} \\ & - \frac{2v_0}{3} \sqrt[3]{1 + \epsilon (-x + x_0)} (3b^2 + x^2)^{\frac{5}{6}} x_0^{\frac{2}{3}} (3b^2 + x_0^2)^{-\frac{5}{6}} x^{-\frac{5}{3}} = 0 . \end{aligned} \quad (42)$$

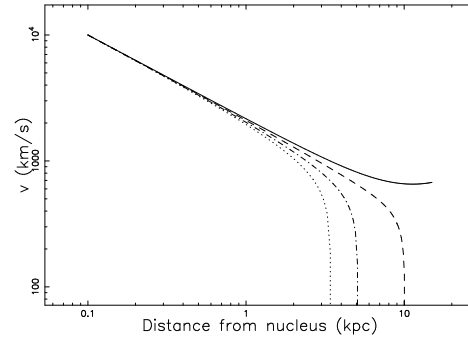


Figure 4. Velocity corrected for radiative losses, i.e. velocity to second order, equation (40), as a function of the distance, with parameters as in Table 1: $\epsilon = 0$ full line, $\epsilon = 1.0 \cdot 10^{-4}$ dashed line, $\epsilon = 2.0 \cdot 10^{-4}$ dot-dash-dot-dash line and $\epsilon = 3.0 \cdot 10^{-4}$ dotted line.

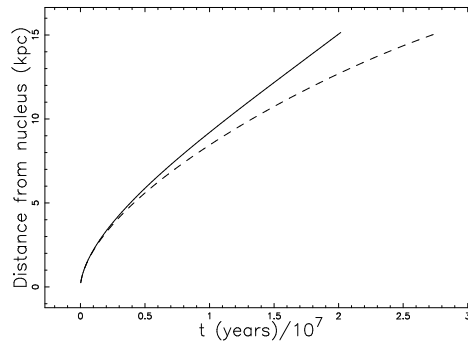


Figure 5. Numerical trajectory corrected for radiative losses as a function of time, with parameters as in Table 1: $\epsilon = 0$ full line and $\epsilon = 8.0 \cdot 10^{-5}$ dashed line.

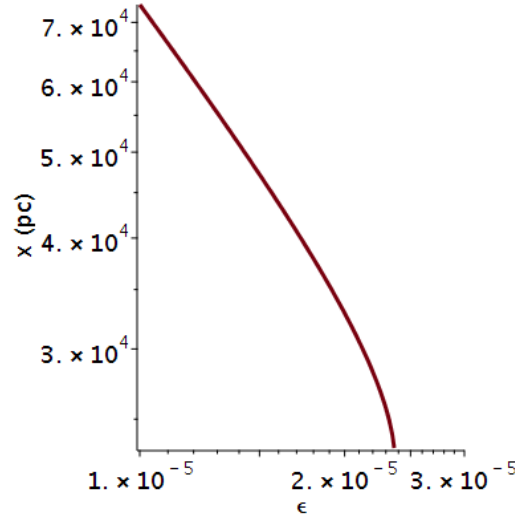


Figure 6. Length of the jet, x_j , in pc as a function of ϵ , with b as in Table 1.

The solution for x of the above minimum determines the jet's length, x_j ,

$$x_j = \frac{4b^2\epsilon^2 + \epsilon^2x_0^2 + \sqrt[3]{D_2}\epsilon x_0 + D_2^{\frac{2}{3}} + 2\epsilon x_0 + \sqrt[3]{D_2} + 1}{4\epsilon\sqrt[3]{D_2}}, \quad (43)$$

where

$$D_1 = -16b^4\epsilon^4 + 429b^2\epsilon^4x_0^2 - 24\epsilon^4x_0^4 + 858b^2\epsilon^3x_0 - 96\epsilon^3x_0^3 + 429b^2\epsilon^2 - 144\epsilon^2x_0^2 - 96\epsilon x_0 - 24, \quad (44)$$

and

$$D_2 = -42b^2\epsilon^3x_0 + \epsilon^3x_0^3 - 42b^2\epsilon^2 + 3\epsilon^2x_0^2 + 2b\sqrt{D_1}\epsilon + 3\epsilon x_0 + 1. \quad (45)$$

Figure 6 shows x_j numerically.

3. Conservation of relativistic flux of energy

The corrections in special relativity (SR) for stable atomic clocks in satellites of the Global Positioning System (GPS) are applied to satellites which are moving at a velocity of $\approx 3.87 \frac{km}{s}$, see [31,32].

In astrophysics we deal with velocities near that of light and therefore we should introduce relativistic conservation laws. The conservation of the relativistic flux of energy in SR in the presence of a velocity v along one direction states that

$$A(x) \frac{1}{1 - \frac{v^2}{c^2}} (e_0 + p_0) v = cost \quad (46)$$

where $A(x)$ is the considered area in the direction perpendicular to the motion, c is the speed of light, $e_0 = c^2\rho$ is the energy density in the rest frame of the moving fluid, and p_0 is the pressure in the rest frame of the moving fluid, see formula A31 in [19] and [11]. In accordance with the current models of classical turbulent jets, we insert $p_0 = 0$. Then the conservation law for the relativistic flux of energy is

$$\rho c^2 v \frac{1}{1 - \frac{v^2}{c^2}} A(x) = \text{const} \quad . \quad (47)$$

In the presence of a Lane–Emden ($n = 5$) density profile, as given by equation (22) and $A(x)$ as given by equation (26), the conservation of relativistic flux of energy for a straight jet takes the form

$$\frac{\rho_0 c^3 \beta \pi x^2 (\tan(\alpha/2))^2}{(1 + \frac{1}{3} \frac{x^2}{b^2})^{5/2} (1 - \beta^2)} = \frac{\rho_0 c^3 \beta_0 \pi x_0^2 (\tan(\alpha/2))^2}{(1 + \frac{1}{3} \frac{x_0^2}{b^2})^{5/2} (1 - \beta_0^2)} \quad , \quad (48)$$

where v is the velocity at x , v_0 is the velocity at x_0 , $\beta = \frac{v}{c}$ and $\beta_0 = \frac{v_0}{c}$. The solution for β to first order is

$$\beta(x; x_0, b, \beta_0) = \frac{N}{(1 + \frac{1}{3} \frac{x_0^2}{b^2})^{5/2} (\beta_0^2 - 1)} \quad , \quad (49)$$

74 where

$$\begin{aligned} N = & 9 \sqrt{3b^2 + x_0^2} x^2 b^4 \beta_0^2 + 6 \sqrt{3b^2 + x_0^2} x^2 b^2 x_0^2 \beta_0^2 + \sqrt{3b^2 + x_0^2} x^2 x_0^4 \beta_0^2 \\ & - 9 \sqrt{3b^2 + x_0^2} x^2 b^4 - 6 \sqrt{3b^2 + x_0^2} x^2 b^2 x_0^2 - \sqrt{3b^2 + x_0^2} x^2 x_0^4 \\ & + \left(243 x^4 (b^2 + \frac{1}{3} x_0^2)^5 \beta_0^4 + (-2 x^4 x_0^{10} - 30 b^2 x^4 x_0^8 - 180 b^4 x^4 x_0^6 \right. \\ & \left. + (972 b^{10} + 1620 b^8 x^2 + 540 b^6 x^4 + 360 b^4 x^6 + 60 b^2 x^8 + 4 x^{10}) x_0^4 \right. \\ & \left. - 810 b^8 x^4 x_0^2 - 486 b^{10} x^4) \beta_0^2 + 243 x^4 (b^2 + \frac{1}{3} x_0^2)^5 \right)^{1/2} . \end{aligned} \quad (50)$$

The equation for the relativistic trajectory is

$$\int_{x_0}^x \frac{1}{\beta(x; x_0, b, \beta_0) c} dx = t \quad . \quad (51)$$

The integral in the above equation does not have an analytical solution and should be integrated numerically. In order to have analytical results, two approximation are now introduced. The first approximation computes a truncated series expansion for the integrand of the integral in equation (51), which transforms the relativistic equation of motion into

$$F(x) - F(x_0) = t \quad , \quad (52)$$

with

$$F(x) = \frac{NF}{162 x_0^2 \beta_0 b^{10} c} \quad , \quad (53)$$

75 where

$$\begin{aligned} NF = & (b^2)^{5/2} x \left(9 \sqrt{3} \sqrt{3b^2 + x_0^2} b^4 \beta_0^2 x^2 + 6 \sqrt{3} \sqrt{3b^2 + x_0^2} b^2 \beta_0^2 x^2 x_0^2 \right. \\ & \left. + \sqrt{3} \sqrt{3b^2 + x_0^2} \beta_0^2 x^2 x_0^4 - 9 \sqrt{3} \sqrt{3b^2 + x_0^2} b^4 x^2 \right. \\ & \left. - 6 \sqrt{3} \sqrt{3b^2 + x_0^2} b^2 x^2 x_0^2 - \sqrt{3} \sqrt{3b^2 + x_0^2} x^2 x_0^4 - 162 \sqrt{b^{10} x_0^4 \beta_0^2} \right) . \end{aligned} \quad (54)$$

76 In the above analytical result we have the time as a function of the distance, see Figure 7 where the
77 percentage error at $x = 15$ kpc is $\delta = 15.91\%$.

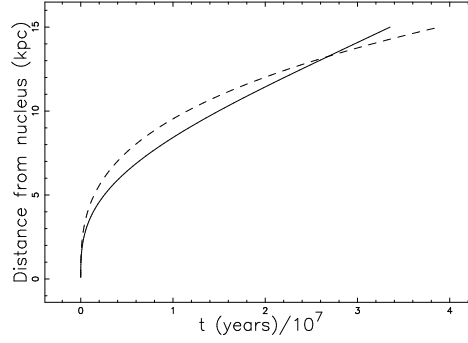


Figure 7. Numerical relativistic solution as given by equation (51) (full line) and truncated series expansion as given by equation (7) (dashed line), with parameters as in Table 2.

Table 2. Parameters for a relativistic extra-galactic jet.

parameter	value
x_0 (pc)	100
β_0	0.9
b (pc)	10000

The second approximation computes a Padé approximant of order [2/1], see [33–35], for the integrand of the integral in equation (51)

$$P(x) - P(x_0) = t \quad , \quad (55)$$

with

$$P(x) = \frac{NP}{162 b^{10} x_0^4 \beta_0^2 c} \quad , \quad (56)$$

78 where

$$\begin{aligned} NP(x) = & -x (b^2)^{5/2} x_0^2 \beta_0 \left(9 \sqrt{3} \sqrt{3b^2 + x_0^2} b^4 \beta_0^2 x^2 \right. \\ & + 6 \sqrt{3} \sqrt{3b^2 + x_0^2} b^2 \beta_0^2 x^2 x_0^2 + \sqrt{3} \sqrt{3b^2 + x_0^2} \beta_0^2 x^2 x_0^4 \\ & - 9 \sqrt{3} \sqrt{3b^2 + x_0^2} b^4 x^2 - 6 \sqrt{3} \sqrt{3b^2 + x_0^2} b^2 x^2 x_0^2 - \sqrt{3} \sqrt{3b^2 + x_0^2} x^2 x_0^4 \\ & \left. - 162 \sqrt{b^{10} x_0^4 \beta_0^2} \right) . \end{aligned} \quad (57)$$

The above equation can be inverted, but the analytical expression for $x = G(t; x_0, \beta_0, b)$ as a function of time is complicated and is omitted here. As an example, with the parameters of Table 2, we have

$$G(t) = \frac{NG}{DG} \quad , \quad (58)$$

79 with

$$\begin{aligned} NG = & -2.9237 \times 10^{-17} \left(-1.7397 \times 10^{54} t - 5.8851 \times 10^{56} \right. \\ & + 2.9816 \times 10^{20} \sqrt{1.9201 \times 10^{73} + 2.3032 \times 10^{70} t} \\ & \left. + 3.4042 \times 10^{67} t^2 \right)^{2/3} + 3.2399 \times 10^{21} \quad , \end{aligned} \quad (59)$$

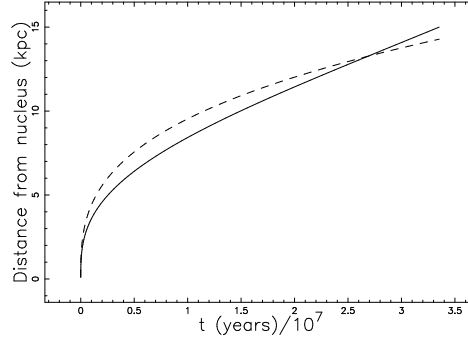


Figure 8. Numerical relativistic solution as given by equation (51) (full line) and Padé approximant as given by equation (8) (dashed line), with parameters as in Table 2.

80 and

$$DG = \left(-1.7397 \times 10^{54} t - 5.8851 \times 10^{56} + 2.9816 \times 10^{20} \sqrt{1.9201 \times 10^{73} + 2.3032 \times 10^{70} t + 3.4042 \times 10^{67} t^2} \right)^{\frac{1}{3}}. \quad (60)$$

81 An example is shown in Figure 8, where the percentage error at $x = 15$ kpc is $\delta = 4.81\%$.

82 3.1. Relativistic solution to second order

We now suppose that the radiative losses are proportional to the relativistic flux of energy. The integral of the losses, L_r , between x_0 and x is

$$L_r(x; x_0, \beta_0, b, c) = -\epsilon \frac{9 (x - x_0) \rho_0 c^3 \beta_0 x_0^2 \pi (\tan(\alpha/2))^2 b^5 \sqrt{3}}{(3b^2 + x_0^2)^{5/2} (1 - \beta_0^2)}. \quad (61)$$

83 The conservation of the relativistic flux of energy in the presence of the back-reaction due to the radiative
84 losses is

$$\frac{NR}{(3b^2 + x^2)^{5/2} (3b^2 + x_0^2)^{5/2} (\beta^2 - 1) (\beta_0^2 - 1)} = \frac{9 \rho_0 \sqrt{3} c^3 \beta_0 x_0^2 b^5}{(3b^2 + x_0^2)^{5/2} (\beta_0^2 - 1)}, \quad (62)$$

85 where

$$NR = 81 \rho_0 b^5 \sqrt{3} \left((b^2 + \frac{1}{3} x^2)^2 \epsilon (\beta + 1) \beta_0 (\beta - 1) (x - x_0) x_0^2 \sqrt{3b^2 + x^2} + (b^2 + \frac{1}{3} x_0^2)^2 \beta x^2 (\beta_0 + 1) (\beta_0 - 1) \sqrt{3b^2 + x_0^2} \right) c^3. \quad (63)$$

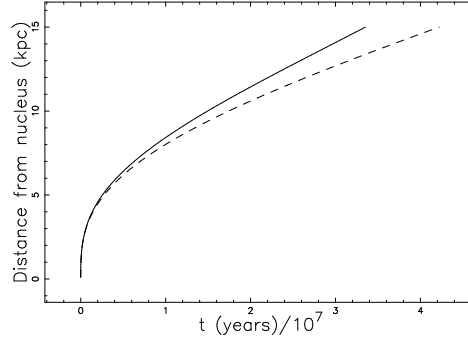


Figure 9. Numerical relativistic solution as given by equation (51) (full line) and solution with back-reaction, i.e. to second order, (dashed line), with parameters as in Table 2 and $\epsilon = 2.0 \cdot 10^{-5}$.

The solution of the above equation, to second order, for β is

$$\beta = \frac{NB}{2(3b^2 + x^2)^{5/2}(\epsilon x - \epsilon x_0 - 1)(3b^2 + x_0^2)x_0^2\beta_0}, \quad (64)$$

where

$$\begin{aligned} NB = & -\sqrt{3b^2 + x_0^2} \left(\sqrt{3b^2 + x_0^2} \times \right. \\ & \left(x^4(\beta_0 - 1)^2(\beta_0 + 1)^2x_0^{10} + 15b^2x^4(\beta_0 - 1)^2(\beta_0 + 1)^2x_0^8 \right. \\ & + (972(b^2 + \frac{1}{3}x^2)^5\beta_0^2\epsilon^2 + 90b^4x^4(\beta_0 - 1)^2(\beta_0 + 1)^2)x_0^6 \\ & - 1944\epsilon(b^2 + \frac{1}{3}x^2)^5\beta_0^2(\epsilon x - 1)x_0^5 + (972(b^2 + \frac{1}{3}x^2)^5\beta_0^2x^2\epsilon^2 \\ & - 1944(b^2 + \frac{1}{3}x^2)^5\beta_0^2x\epsilon + 4x^{10}\beta_0^2 + 60b^2x^8\beta_0^2 + 360b^4x^6\beta_0^2 \\ & + 270b^6(\beta_0^2 + 1)^2x^4 + 1620b^8x^2\beta_0^2 + 972b^{10}\beta_0^2)x_0^4 \\ & \left. + 405b^8x^4(\beta_0 - 1)^2(\beta_0 + 1)^2x_0^2 + 243b^{10}x^4(\beta_0 - 1)^2(\beta_0 + 1)^2 \right)^{1/2} \\ & \left. + 27(b^2 + \frac{1}{3}x_0^2)^3(\beta_0 + 1)x^2(\beta_0 - 1) \right). \quad (65) \end{aligned}$$

The relativistic equation of motion with back-reaction can be solved by numerically integrating the relation in equation (51). Figure 9 gives an example.

4. Astrophysical applications

We now analyse two models for the synchrotron emission along the jet.

4.1. Direct conversion

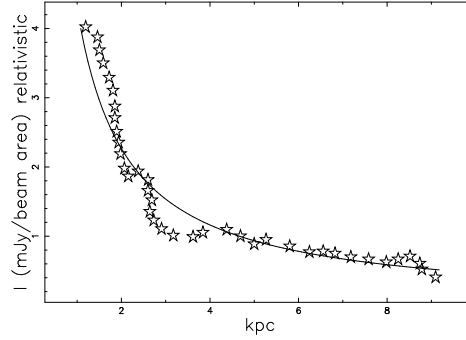


Figure 10. Observed intensity profile along the centreline of 3C31 (empty stars) and theoretical intensity as given by equation (67), with parameters as in Table 2 (full line). The observational percentage of reliability is $\epsilon_{\text{obs}} = 86.19\%$.

The flux of observed radiation along the centre of the jet, I_c , in the classical case is assumed to scale as

$$I_c(x; x_0, v_0, b, \epsilon) \propto \frac{L(x; x_0, v_0, b, \epsilon)}{x^2}, \quad (66)$$

where L , the sum of the radiative losses, is given by equation (38).

The above relation connects the observed intensity of radiation with the rate of energy transfer per unit area. In the relativistic case

$$I_c(x; x_0, \beta_0, b, c) \propto \frac{L_r(x; x_0, \beta_0, b, c)}{x^2}, \quad (67)$$

where L_r is given by equation (61)

A statistical test for the the goodness of fit is the observational percentage of reliability, ϵ_{obs} ,

$$\epsilon_{\text{obs}} = 100 \left(1 - \frac{\sum_j |I_{\text{obs}} - I_{\text{theo}}|_j}{\sum_j I_{\text{theo},j}} \right). \quad (68)$$

In order to make a comparison with the observed profile of intensity, we chose 3C31, see Figure 8 in [7]; Figure 10 shows the theoretical synchrotron intensity as well as the observed one.

4.2. The magnetic field of equipartition

The magnetic field in CGS has an energy density of $\frac{B^2}{8\pi}$ where B is the magnetic field. The presence of the magnetic field can be modeled assuming equipartition between the kinetic energy and the magnetic energy

$$\frac{B(x)^2}{8\pi} = \frac{1}{2} \rho v^2. \quad (69)$$

Inserting the above equation in the classical equation for the conservation of the flux of energy (27), a factor 2 will appear on both sides of the equation, leaving unchanged the result for the deduction of the velocity to first order. The magnetic field as a function of the distance x when the velocity is given by equation (29) and in the presence of a Lane–Emden ($n = 5$) profile for the density is

$$B(x; x_0, b) = \frac{B_0 (3b^2 + x_0^2)^{\frac{5}{12}} x_0^{\frac{2}{3}}}{(3b^2 + x^2)^{\frac{5}{12}} x^{\frac{2}{3}}}. \quad (70)$$

where B_0 is the magnetic field at $x = x_0$. We assume an inverse power law spectrum for the ultrarelativistic electrons, of the type

$$N(E)dE = KE^{-p}dE \quad (71)$$

where K is a constant and p the exponent of the inverse power law. The intensity of the synchrotron radiation has a standard expression, as given by formula (1.175) in [36],

$$I(\nu) \approx 0.933 \times 10^{-23} \alpha_p(p) K l H_{\perp}^{(p+1)/2} \left(\frac{6.26 \times 10^{18}}{\nu} \right)^{(p-1)/2} \quad (72)$$

$erg \ sec^{-1} cm^{-2} Hz^{-1} rad^{-2}$

where ν is the frequency, H_{\perp} is the magnetic field perpendicular to the electron's velocity, l is the dimension of the radiating region along the line of sight, and $\alpha_p(p)$ is a slowly varying function of p which is of the order of unity. We now analyse the intensity along the centreline of the jet, which means that the radiating length is

$$l(x; \alpha) = x \tan\left(\frac{\alpha}{2}\right) \quad (73)$$

The intensity, assuming a constant p , scales as

$$I(x; x_0, p) = \frac{I_0 B_0^{\frac{p}{2} + \frac{1}{2}} x}{B_0^{\frac{p}{2} + \frac{1}{2}} x_0} \quad (74)$$

where I_0 is the intensity at $x = x_0$ and B_0 the magnetic field at $x = x_0$. We insert Eq. (70) in order to have an analytical expression for the centreline intensity

$$I(x; x_0, p, b) = (3b^2 + x_0^2)^{\frac{5p}{24} + \frac{5}{24}} i_0 x^{-\frac{p}{3} + \frac{2}{3}} x_0^{\frac{p}{3} - \frac{2}{3}} (3b^2 + x^2)^{-\frac{5p}{24} - \frac{5}{24}} \quad (75)$$

The above equation for the intensity is relative to the unit area; in order to have the intensity on the centreline, I_c , we should make a further division by the area of interest, which scales $\propto x^2$

$$I_c(x; x_0, p, b) = \frac{I(x; x_0, p, b)}{x^2} \quad (76)$$

Figure 11 shows the theoretical synchrotron intensity with the variable magnetic field as well as the observed one for 3C31.

5. Conclusions

Classical case The approximate trajectory of a turbulent jet in the presence of a Lane–Emden ($n = 5$) medium has been evaluated to first order, see equation (35). The solution for the velocity to first order allows the insertion of the back-reaction, i.e. the radiative losses, in the equation for the flux of energy conservation, see equation (39), and as a consequence the velocity corrected to second order, see equation (40). The trajectory, calculated numerically to second order, is shown in Figure 5. The radiative losses allow evaluating the length at which the advancing velocity of the jet is zero. This length has a complicated analytical expression and was presented numerically, see Figure 6.

Relativistic case In the relativistic case it is possible to derive an analytical expression for β to first order, see equation (49), and to second order (taking into account radiative losses), see equation (64).

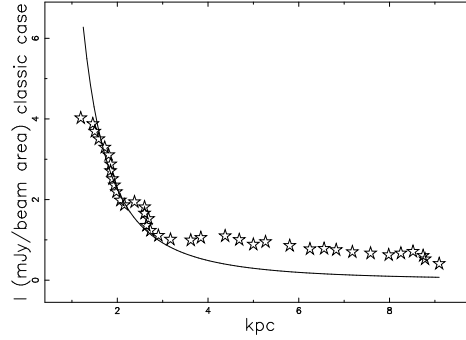


Figure 11. Observed intensity profile along the centreline, I_c , of 3C31 (empty stars) and theoretical intensity as given by equation (76), with parameters as in Table 1. The observational percentage of reliability is $\epsilon_{\text{obs}} = 73.79\%$.

The relativistic trajectory to first order has been evaluated through a series, see equation (52) or a Padé approximant of order [2/1], see equation (58). The relativistic equation of motion to second order (back-reaction) has been evaluated numerically, see Figure 9. In other words, with the introduction of the radiative losses, the length of the classical or relativistic jet becomes finite rather than infinite.

An astrophysical application The radiative losses are represented by equation (37) in the classical case and by (61) in the relativistic case. A division of the two above quantities by the area of interest allows deriving the theoretical rate of energy transfer per unit area, which can be compared with the intensity of radiation along the jet, for example, 3C31, see Figure 10. The spatial behaviour of the magnetic field is introduced under the hypothesis of equipartition between the kinetic and magnetic energy, see equation (70), and this allows closing the standard equation for the synchrotron emissivity, see equation (73).

References

1. Curtis, H.D. Descriptions of 762 Nebulae and Clusters Photographed with the Crossley Reflector. *Publications of Lick Observatory* **1918**, *13*, 9–42.
2. Fanaroff, B.L.; Riley, J.M. The morphology of extragalactic radio sources of high and low luminosity. *MNRAS* **1974**, *167*, 31P–36P.
3. Kembhavi, A.K.; Narlikar, J.V. *Quasars and active galactic nuclei : an introduction*; Cambridge University Press: Cambridge, 1999.
4. Bridle, A.H.; Perley, R.A. Extragalactic Radio Jets. *ARA&A* **1984**, *22*, 319–358.
5. Liu, F.K.; Zhang, Y.H. A new list of extra-galactic radio jets. *A&A* **2002**, *381*, 757–760, [\[astro-ph/0212477\]](#).
6. Hardcastle, M.J.; Sakelliou, I. Jet termination in wide-angle tail radio sources. *MNRAS* **2004**, *349*, 560–575.
7. Laing, R.A.; Bridle, A.H. Relativistic models and the jet velocity field in the radio galaxy 3C 31. *MNRAS* **2002**, *336*, 328–352.

- 136 8. Nawaz, M.A.; Wagner, A.Y.; Bicknell, G.V.; Sutherland, R.S.; McNamara, B.R. Jet-intracluster
137 medium interaction in Hydra A - I. Estimates of jet velocity from inner knots. *MNRAS* **2014**,
138 *444*, 1600–1614, [[1408.4512](#)].
- 139 9. Nawaz, M.A.; Bicknell, G.V.; Wagner, A.Y.; Sutherland, R.S.; McNamara, B.R. Jet-intracluster
140 medium interaction in Hydra A - II. The effect of jet precession. *MNRAS* **2016**, *458*, 802–815,
141 [[1602.02969](#)].
- 142 10. Zaninetti, L. Classical and relativistic conservation of momentum flux in radio-galaxies . *Applied*
143 *Physics Research* **2015**, *7*, 43–62.
- 144 11. Zaninetti, L. Classical and Relativistic Flux of Energy Conservation in Astrophysical Jets.
145 *Journal of High Energy Physics, Gravitation and Cosmology* **2016**, *1*, 41–56.
- 146 12. Kellermann, K.I.; Richards, E.A. Radio Observations of the Hubble Deep Field. The Hubble
147 Deep Field; Livio, M.; Fall, S.M.; Madau, P., Eds.; Cambridge University Press: Cambridge,
148 1998; p. 60.
- 149 13. Bird, R.; Stewart, W.; Lightfoot, E. *Transport Phenomena ; second Edition*; John Wiley and
150 Sons: New York, 2002.
- 151 14. Landau, L. *Fluid Mechanics 2nd edition*; Pergamon Press: London, 1987.
- 152 15. Goldstein, S. *Modern Developments in Fluid Dynamics*; Dover: New York, 1965.
- 153 16. Reichardt, V. Gesetzmäßigkeiten der freien Turbulenz. *VDI-Forschungsheft* **1942**, *414*, 141.
- 154 17. Reichardt, V. Vollständige Darstellung der turbulenten Geschwindigkeitsverteilung in glatten
155 Leitungen. *Zeitschrift für Angewandte Mathematik und Mechanik* **1951**, *31*, 208–219.
- 156 18. Schlichting, H. *Boundary Layer Theory*; McGraw-Hill: New York, 1979.
- 157 19. De Young, D.S. *The physics of extragalactic radio sources*; University of Chicago Press:
158 Chicago, 2002.
- 159 20. Laing, R.A.; Bridle, A.H. Adiabatic relativistic models for the jets in the radio galaxy 3C 31.
160 *MNRAS* **2004**, *348*, 1459–1472, [[astro-ph/0311499](#)].
- 161 21. Lane, H.J. On the Theoretical Temperature of the Sun, under the Hypothesis of a gaseous Mass
162 maintaining its Volume by its internal Heat, and depending on the laws of gases as known to
163 terrestrial Experiment. *American Journal of Science* **1870**, *148*, 57–74.
- 164 22. Emden, R. *Gaskugeln: anwendungen der mechanischen warmetheorie auf kosmologische und*
165 *meteorologische probleme*; B. Teubner.: Berlin, 1907.
- 166 23. Chandrasekhar, S. *An introduction to the study of stellar structure*; Dover: New York, 1967.
- 167 24. Binney, J.; Tremaine, S. *Galactic dynamics, Second Edition*; Princeton University Press:
168 Princeton, NJ, 2011.
- 169 25. Zwillinger, D. *Handbook of differential equations*; Academic Press: New York, 1989.
- 170 26. Hansen, C.J.; Kawaler, S.D. *Stellar Interiors. Physical Principles, Structure, and Evolution.*;
171 Springer-Verlag: Berlin, 1994.
- 172 27. Abramowitz, M.; Stegun, I.A. *Handbook of Mathematical Functions with Formulas, Graphs,*
173 *and Mathematical Tables*; Dover: New York, 1965.
- 174 28. von Seggern, D. *CRC Standard Curves and Surfaces*; CRC: New York, 1992.
- 175 29. Thompson, W.J. *Atlas for computing mathematical functions*; Wiley-Interscience: New York,
176 1997.

- 177 30. Olver, F.W.J.e.; Lozier, D.W.e.; Boisvert, R.F.e.; Clark, C.W.e. *NIST handbook of mathematical*
178 *functions.*; Cambridge University Press. : Cambridge, 2010.
- 179 31. Ashby, N. Relativity in the Global Positioning System. *Living Reviews in Relativity* **2003**, *6*, 1.
- 180 32. Ashby, N.; Nelson, R.A. GPS, Relativity, and Extraterrestrial Navigation. IAU Symposium
181 #261, American Astronomical Society, 2009, Vol. 261, p. 889.
- 182 33. Adachi, M.; Kasai, M. An Analytical Approximation of the Luminosity Distance in
183 Flat Cosmologies with a Cosmological Constant. *Progress of Theoretical Physics* **2012**,
184 *127*, 145–152, [[arXiv:astro-ph.CO/1111.6396](https://arxiv.org/abs/astro-ph.CO/1111.6396)].
- 185 34. Aviles, A.; Bravetti, A.; Capozziello, S.; Luongo, O. Precision cosmology with Padé rational
186 approximations: Theoretical predictions versus observational limits. *Phys. Rev. D* **2014**,
187 *90*, 043531, [[arXiv:gr-qc/1405.6935](https://arxiv.org/abs/gr-qc/1405.6935)].
- 188 35. Wei, H.; Yan, X.P.; Zhou, Y.N. Cosmological applications of Pade approximant. *Journal of*
189 *Cosmology and Astroparticle Physic* **2014**, *1*, 45, [[arXiv:astro-ph.CO/1312.1117](https://arxiv.org/abs/astro-ph.CO/1312.1117)].
- 190 36. Lang, K.R. *Astrophysical formulae. (Second Edition)*; Springer: New York, 1980.

191 © March 10, 2024 by the author; submitted to *Galaxies* for possible open access
192 publication under the terms and conditions of the Creative Commons Attribution license
193 <http://creativecommons.org/licenses/by/4.0/>.